

## Mechanism for Binding to the Flexible Cavity of Permethylated $\alpha$ -Cyclodextrin

KOJI KANO,\* TAIZO ISHIMURA and SHIGERU NEGI

*Department of Molecular Science and Technology, Faculty of Engineering, Doshisha University, Tanabe, Kyoto 610-03, Japan.*

(Received: 23 June 1995)

**Abstract.** The cavity of  $\alpha$ -cyclodextrin ( $\alpha$ -CDx) is too small to include *o*-toluic acid (*o*-TA) while it is filled by *p*-toluic acid (*p*-TA) to form a relatively stable inclusion complex. Such strict selectivity is ascribed to a rigid structure of the  $\alpha$ -CDx cavity which is stabilized by intramolecular hydrogen bonds between the O(2) hydroxyl groups and the O(3) hydroxyl groups of adjacent glucopyranose units. Meanwhile, the substrate selectivity of hexakis(2,3,6-tri-*O*-methyl)- $\alpha$ -CDx (TMe- $\alpha$ -CDx) remains somewhat obscure because of the flexible nature of its cavity. The absence of the intramolecular hydrogen bonds seems to cause the flexible nature of the TMe- $\alpha$ -CDx cavity leading to an induced-fit type inclusion. The structures of the inclusion complexes have been presented on the basis of the  $^1\text{H}$  NMR data. The thermodynamic parameters indicate that the complexation of TMe- $\alpha$ -CDx with *o*-TA or *p*-TA is the entropically favorable process. The entropically favorable complexation of TA with TMe- $\alpha$ -CDx seems to occur through dehydration from the  $\text{CO}_2\text{H}$  group of TA which is situated at the hydrophobic CDx cavity. The dipole–dipole interaction has been regarded as the force which dominates the orientation of the polar guest molecule in the CDx cavity.

**Key words.** Permethylated  $\alpha$ -cyclodextrin, toluic acids, flexible cavity, induced-fit type inclusion,  $^1\text{H}$  NMR, thermodynamic parameters, dehydration, dipole–dipole interaction.

### 1. Introduction

Permethylated cyclodextrins are expected to have unique properties different from those of native cyclodextrins (CDxs). Several studies on permethylated CDxs have been reported. The X-ray analyses indicate that the macrocyclic structure of permethylated CDx is distorted more extensively than the corresponding native CDx [1]. The absence of the intramolecular hydrogen bonds causes the flexible nature of the cavity of permethylated CDx. The difference in the crystal structures between the hexakis(2,3,6-tri-*O*-methyl)- $\alpha$ -CDx (TMe- $\alpha$ -CDx) complexes of (*S*)- and (*R*)-mandelic acids has been interpreted in terms of the induced-fit type inclusion in the TMe- $\alpha$ -CDx cavity [2]. In some cases, the orientations of guest molecules in the crystal structures of TMe- $\alpha$ -CDx differ from those of  $\alpha$ -CDx [3]. The orientation of guest molecule in a crystal is not always consistent with that in solution [4]. The thermodynamic parameters for complexation of TMe- $\alpha$ -CDx with various substituted benzenes have been determined [5]. In most cases, the

\* Author for correspondence.

complexation is the enthalpically favorable and entropically unfavorable process. The main force for forming inclusion complexes of TMe- $\alpha$ -CDx with benzoic acid, hydroxybenzoic acids, nitrophenols, nitroanilines, and so on has been assumed to be the van der Waals interaction, not hydrophobic interaction [5]. Similar results have also been obtained for formation of inclusion complexes of  $\alpha$ - or  $\beta$ -CDx and substituted benzenes [6–8]. We measured the thermodynamic parameters for complexation of 3-(*p*-hydroxyphenyl)-1-propanol with  $\beta$ -CDx, heptakis(2,6-di-*O*-methyl)- $\beta$ -CDx (DMe- $\beta$ -CDx), and heptakis(2,3,6-tri-*O*-methyl)- $\beta$ -CDx (TMe- $\beta$ -CDx) [9]. In both cases of  $\beta$ -CDx and DMe- $\beta$ -CDx, the negative and relatively small enthalpy change ( $\Delta H$ ) and positive entropy change ( $\Delta S$ ) promote the inclusion.

Meanwhile, a negative and relatively large  $\Delta S$  is measured for complexation of TMe- $\beta$ -CDx. The favorable van der Waals interaction and the strict reduction in rotational freedom of the OCH<sub>3</sub> groups of the host upon complexation can explain the thermodynamic parameters obtained for the TMe- $\beta$ -CDx complex. In the present study, we measured the thermodynamic parameters for complexation of *o*- (*o*-TA) and *p*-toluic acids (*p*-TA) with TMe- $\alpha$ -CDx and the <sup>1</sup>H NMR spectra of these complexes to elucidate the mechanism for formation of the inclusion complexes. There are two points in the present study. One is proof of induced-fit type inclusion in the TMe- $\alpha$ -CDx cavity in solution; the other is dipole–dipole interaction as a force which determines the orientation of a guest molecule in the CDx cavity.

## 2. Experimental

$\alpha$ -CDx, *o*-TA, and *p*-TA (reagent grade, Nacalai) were purchased and used without further purification. TMe- $\alpha$ -CDx was prepared by Hakomori's method [10].

The absorption spectra were recorded on a Shimadzu UV-2100 spectrophotometer whose cell holder was thermostatted. The <sup>1</sup>H NMR spectra (400 MHz) were recorded on a JEOL JNM-A400 spectrometer at 23 ± 0.5 °C. The chemical shifts were determined using HDO as an internal standard ( $\delta_{\text{HDO}}$  4.650 ppm).

The binding constants (*K*) were determined in 0.2 mol dm<sup>−3</sup> HCl–KCl buffer solutions at pH 2.0.

The dipole moments of  $\alpha$ -CDx and TMe- $\alpha$ -CDx were calculated using the MOPAC program (version 6 developed by J. J. P. Stewart, US Airforce Academy, USA) on a COMTEC 4D RPC XS24Z R4000 workstation.

## 3. Results and Discussion

The binding constants (*K*) for complexation in water at pH 2.0 were determined by the literature method using absorption spectral changes of guests upon addition of CDx [11]. A typical example of the absorption spectral change is shown in Figure 1. The isosbestic points were observed in each system, indicating the formation of

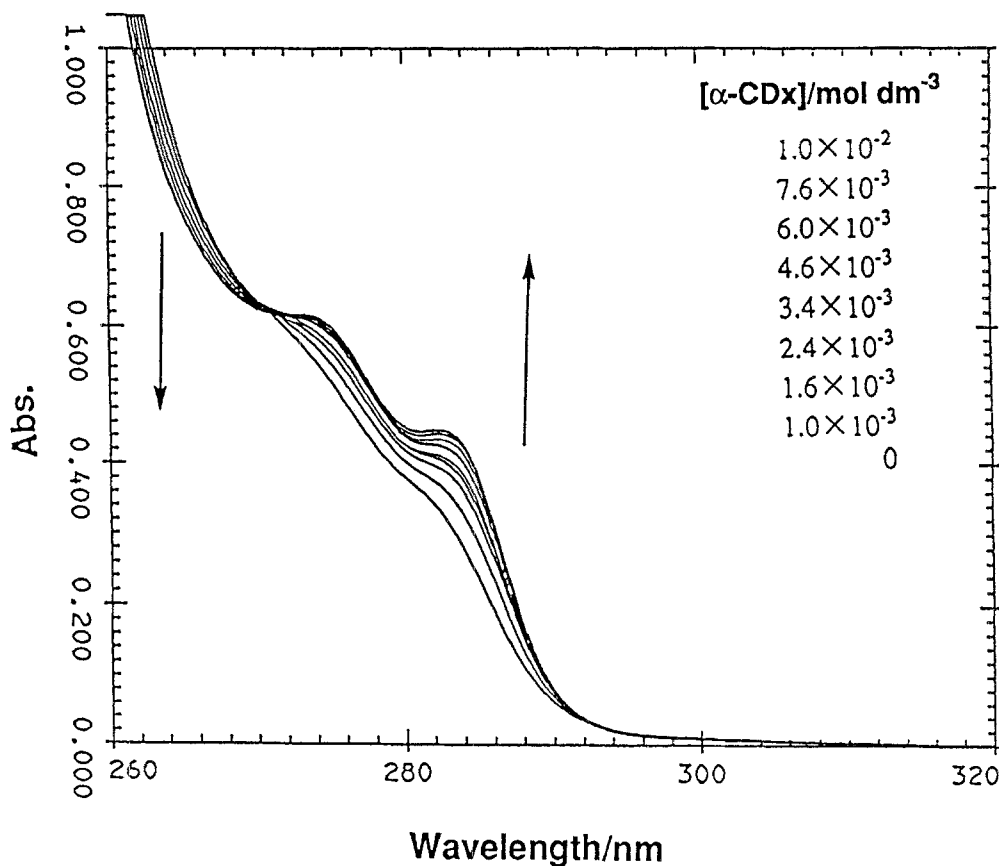
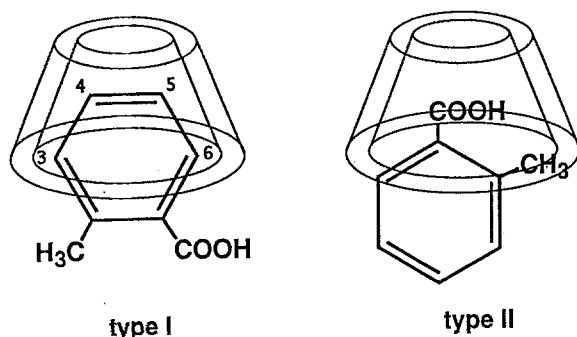


Fig. 1. Absorption spectral change of *p*-TA ( $5 \times 10^{-4} \text{ mol dm}^{-3}$ ) upon addition of  $\alpha$ -CDx in water at pH 2.0 and 25 °C.

the 1 : 1 host–guest complex. The  $K$  values determined are summarized in Table I. No appreciable spectral change was observed in the *o*-TA- $\alpha$ -CDx system, clearly indicating that *o*-TA is not included in the  $\alpha$ -CDx cavity. The  $^1\text{H}$  NMR measurements also support the absence of the interaction between *o*-TA and  $\alpha$ -CDx. The size of *o*-TA seems to be too large to be included in the  $\alpha$ -CDx cavity. In contrast, *o*-TA complexes with TMe- $\alpha$ -CDx. TMe- $\alpha$ -CDx without intramolecular hydrogen bonds can transform the shape of its cavity to form an inclusion complex of the guest having a relatively large molecular-size. It is assumed that *o*-TA is included in the TMe- $\alpha$ -CDx cavity through an induced-fit type host–guest interaction. Let us assume two types of complexes of *o*-TA and TMe- $\alpha$ -CDx as exhibited in Figure 2. Judging from the CPK molecular model, the formation of the type I complex seems to be plausible. In the case of the type II complex, *o*-TA cannot penetrate deeply into the TMe- $\alpha$ -CDx cavity because of the steric hindrance due to the  $\text{CH}_3$  group.

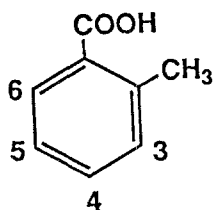
TABLE I. The  $K$  values as a function of temperature and the enthalpy ( $\Delta H$ ) and entropy changes ( $\Delta S$ ) for complexation.

Host	Guest	Temp. (K)	$K$ (dm <sup>3</sup> mol <sup>-1</sup> )	$\Delta H$ (kJ mol <sup>-1</sup> )	$\Delta S$ (J mol <sup>-1</sup> K <sup>-1</sup> )
$\alpha$ -CDx	<i>o</i> -TA	298	0	—	—
TMe- $\alpha$ -CDx	<i>o</i> -TA	288	318	-11.5	+8.1
		293	307		
		298	270		
		303	249		
		308	234		
$\alpha$ -CDx	<i>p</i> -TA	288	1233	-34.8	-27.1
		293	998		
		298	819		
		303	685		
		308	595		
TMe- $\alpha$ -CDx	<i>p</i> -TA	288	1921	-7.1	+38.2
		293	1852		
		298	1767		
		303	1671		
		308	1589		

Fig. 2. Models of the inclusion complex of *o*-TA and transformed TMe- $\alpha$ -CDx.

With *p*-TA, both  $\alpha$ -CDx and TMe- $\alpha$ -CDx form relatively stable complexes. It is clear, therefore, that the misfit of the molecular sizes prohibits the complexation of *o*-TA with  $\alpha$ -CDx.

In order to determine the structures of the complexes, the  $^1\text{H}$  NMR titrations were carried out. As mentioned above, no appreciable shifts of both host and guest signals were observed in the *o*-TA- $\alpha$ -CDx system. The changes in the  $^1\text{H}$  NMR signals of *o*-TA upon addition of TMe- $\alpha$ -CDx are shown in Figures 3 and 4. All signals due to *o*-TA shift to lower magnetic-fields upon addition of TMe- $\alpha$ -CDx. The most remarkable shift occurs for the proton at the 6-position. The proton at the



[TMe- $\alpha$ -CDx] / mol dm<sup>-3</sup>

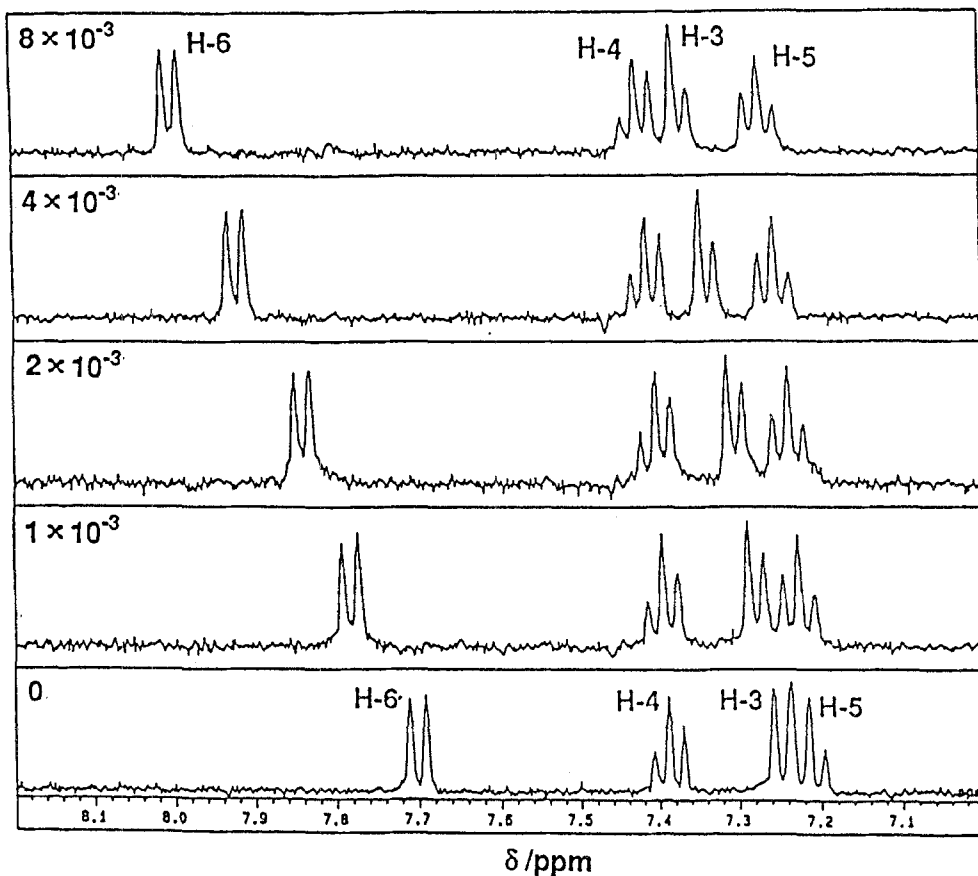


Fig. 3. Changes in the <sup>1</sup>H NMR spectrum of *o*-TA (1 × 10<sup>-3</sup> mol dm<sup>-3</sup>) upon addition of TMe- $\alpha$ -CDx in D<sub>2</sub>O at pD 2.0.

3-position and the methyl protons at the 2-position of *o*-TA shift to an intermediate extent. The protons at the 4- and 5-positions slightly shift to lower magnetic-fields. Such results on the NMR titration can be explained reasonably by the type I complex in Figure 2. The protons at the 3- and 6-positions of *o*-TA of the type I complex will contact with the wall of the transformed TMe- $\alpha$ -CDx leading to a van der Waals effect in the <sup>1</sup>H NMR of these protons. Since the protons at the 4- and

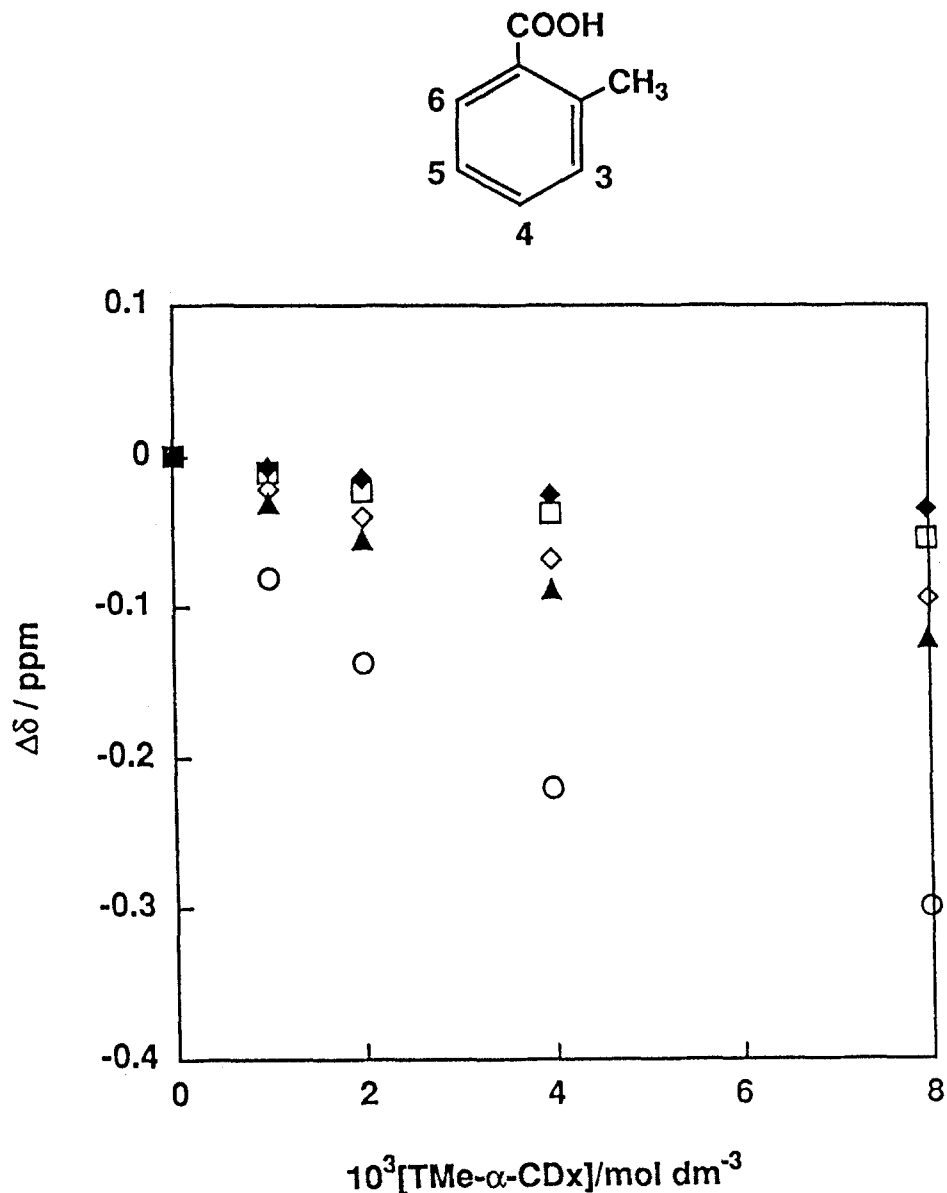


Fig. 4. Changes in the chemical shifts of *o*-TA ( $1 \times 10^{-3} \text{ mol dm}^{-3}$ ) upon addition of TMe- $\alpha$ -CDx in D<sub>2</sub>O at pD 2.0. ▲: H3; ◆: H4; □: H5; ○: H6; ◇: CH<sub>3</sub>.

5-positions of *o*-TA are located at the narrower side of the cavity without significant contact with the CDx wall, the signals due to these protons should slightly shift upon complexation. The CPK molecular model indicates that the type II complex is a very shallow complex and predicts that the signals due to the protons at the 3, 4, and 5 positions scarcely shift upon complexation with TMe- $\alpha$ -CDx. It can be

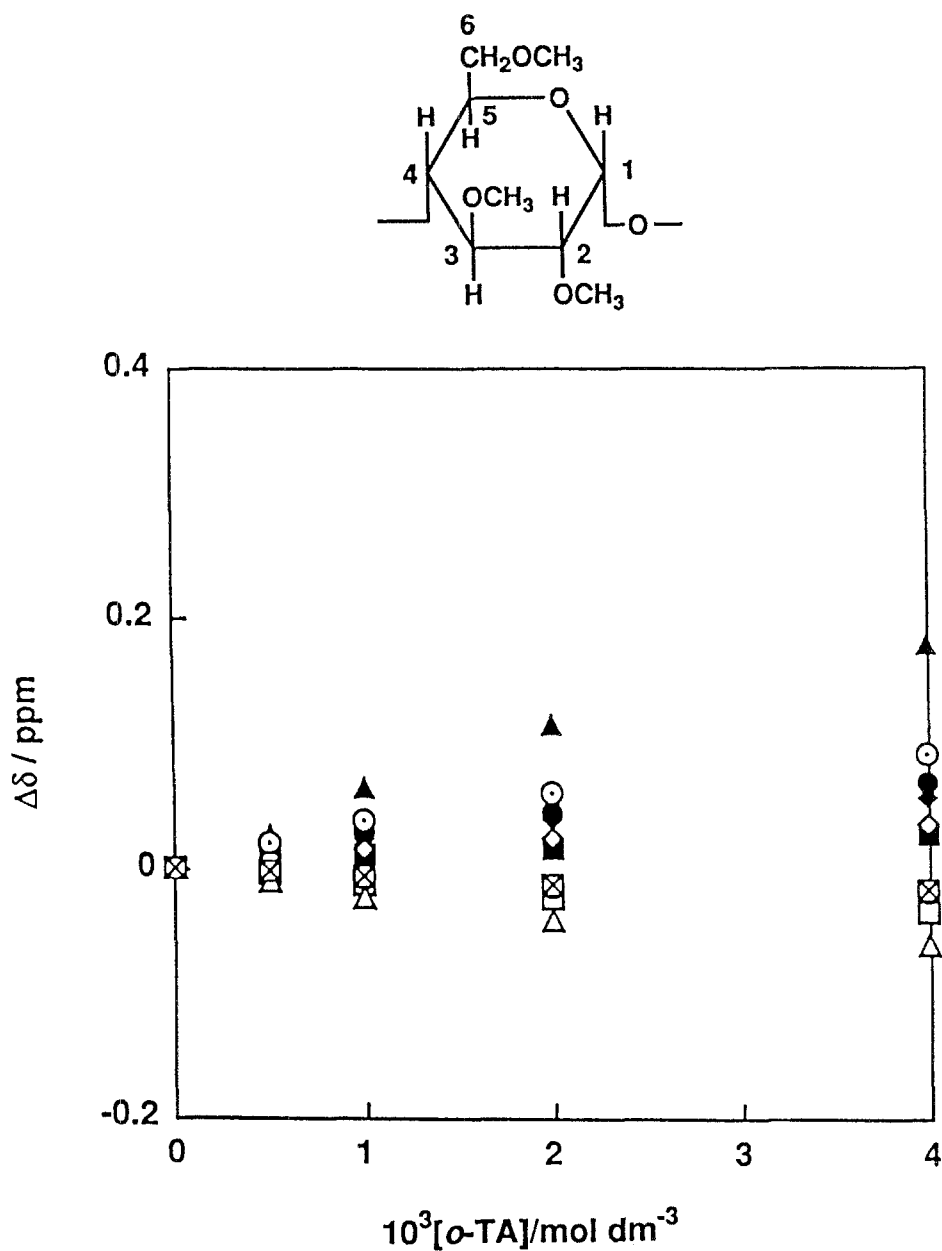


Fig. 5. Changes in the chemical shifts of TMe- $\alpha$ -CDx ( $1 \times 10^{-3} \text{ mol dm}^{-3}$ ) upon addition of *o*-TA in  $\text{D}_2\text{O}$  at pD 2.0. ■: H-1; ●: H-2; ▲: H-3; ◆: H-4; □: H-5; ○: H-6; △: H-6'; ◇: CH<sub>3</sub>-2; ⊙: CH<sub>3</sub>-3; ⊠: CH<sub>3</sub>-6.

concluded, therefore, that the type I complex is formed in this system. The shifts in the signals due to TMe- $\alpha$ -CDx upon addition of *o*-TA are shown in Figure 5. The signals due to the protons at the 1-, 2-, 3-, and 4-positions of TMe- $\alpha$ -CDx shift to

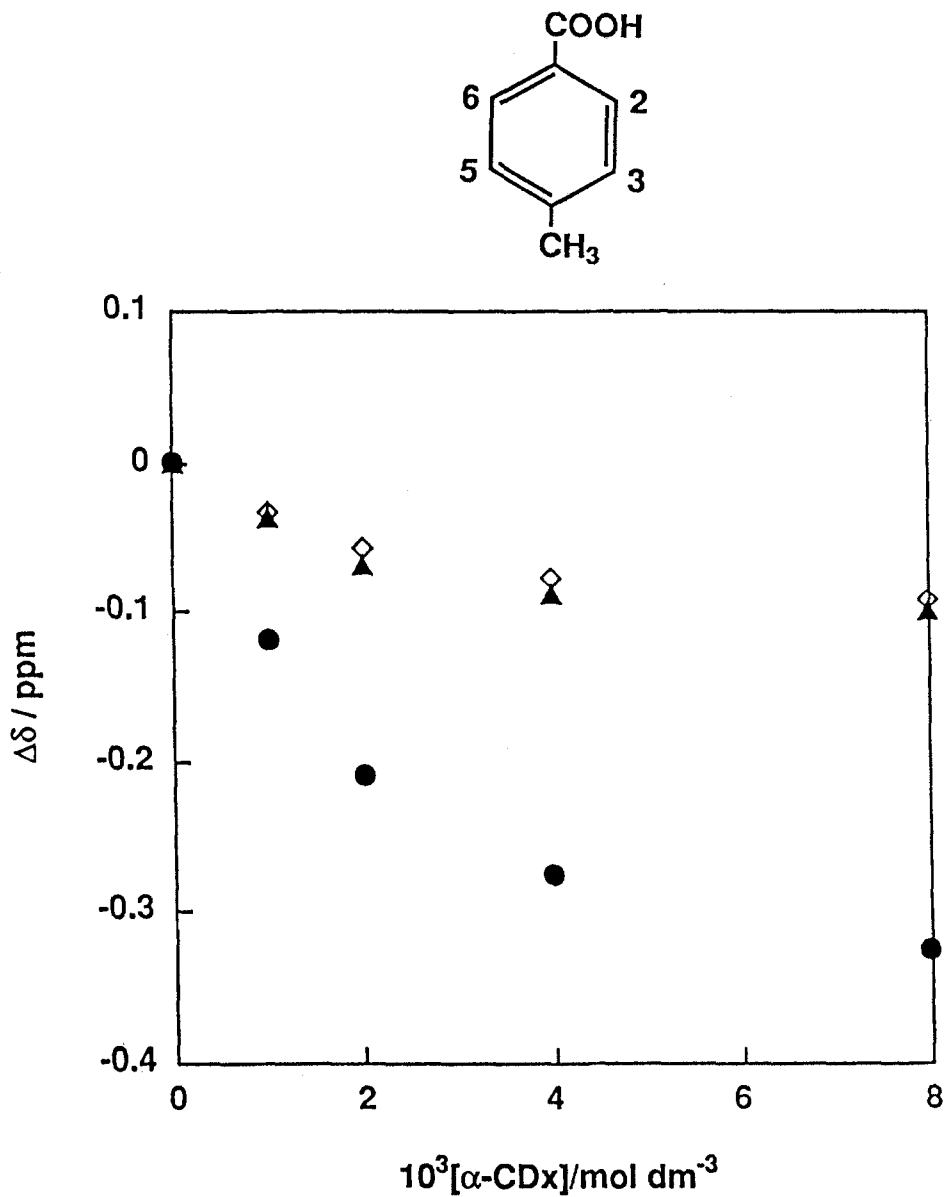
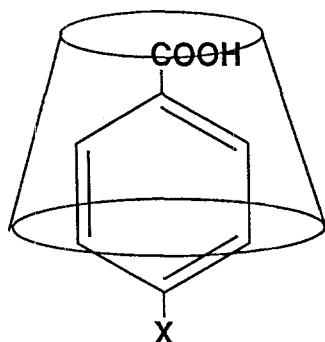


Fig. 6. Changes in the chemical shifts of *p*-TA ( $1 \times 10^{-3} \text{ mol dm}^{-3}$ ) upon addition of  $\alpha$ -CDx in  $\text{D}_2\text{O}$  at pD 2.0. ●: H2, H6; ▲: H3, H5; ◇: CH<sub>3</sub>.

higher magnetic fields while those due to the protons at the 5- and 6-positions shift to lower magnetic fields upon addition of *o*-TA. These results are clearly explained by the anisotropic effect of the benzene ring in the type I complex. *o*-TA penetrates





**type III**

Fig. 7. A model of the inclusion complex of CDx and *p*-substituted benzoic acid.

into the TMe- $\alpha$ -CDx cavity from the wider side of the cavity as shown in Figure 2. The ROESY spectrum was measured for the *o*-TA ( $4 \times 10^{-3}$  M)-TMe- $\alpha$ -CDx ( $2 \times 10^{-3}$  M) system. A correlation between all protons of *o*-TA and the methyl protons at the 3-positions of TMe- $\alpha$ -CDx was observed. Such correlation is possible in the type I complex. In the case of the type II complex, no correlation should be observed between the methyl protons at the 3-position of TMe- $\alpha$ -CDx and the protons at the 3- and 4-positions of *o*-TA.

All proton signals of *p*-TA also shift to lower magnetic-fields upon addition of  $\alpha$ -CDx as shown in Figure 6. The shifts in the signals due to the protons at the 2- and 6-positions of *p*-TA are more remarkable than those at the 3- and 5-positions and the signal due to the methyl protons at the 4-position. These results clearly exhibit that the 2- and 6-positions of *p*-TA are situated at a narrower part of the  $\alpha$ -CDx cavity and the 3- and 5-positions are located at the wider part of the cavity. The structure of the *p*-TA- $\alpha$ -CDx complex estimated from the  $^1\text{H}$  NMR titration is shown in Figure 7. In the type III complex, the polar  $\text{CO}_2\text{H}$  group is located at the hydrophobic cavity and the hydrophobic methyl group of *p*-TA is exposed to the aqueous bulk phase. Such a novel structure has already been assumed for the benzoic acid- $\alpha$ -CDx complex on the basis of the  $^1\text{H}$  NMR data [12]. The X-ray analysis has also revealed the formation of the type III complex of *p*-hydroxybenzoic acid and  $\alpha$ -CDx [13]. However, the reverse orientation of benzoic acid in the  $\alpha$ -CDx cavity has been presented from the  $^{13}\text{C}$  NMR data [14]. The present results strongly suggest the formation of the type III complex of *p*-TA and  $\alpha$ -CDx. The dipole moments of  $\alpha$ -CDx and TMe- $\alpha$ -CDx, which were calculated using MOPAC software, are shown in Figure 8. If the orientation of *p*-TA in the CDx cavity is dominated by a dipole-dipole interaction, it is quite reasonable that the type III complex shown in Figure 7 is formed. The important role of the dipole-dipole interaction in formation of inclusion complexes has been demonstrated [12, 15]. The changes in the chemical shifts of  $\alpha$ -CDx upon addition

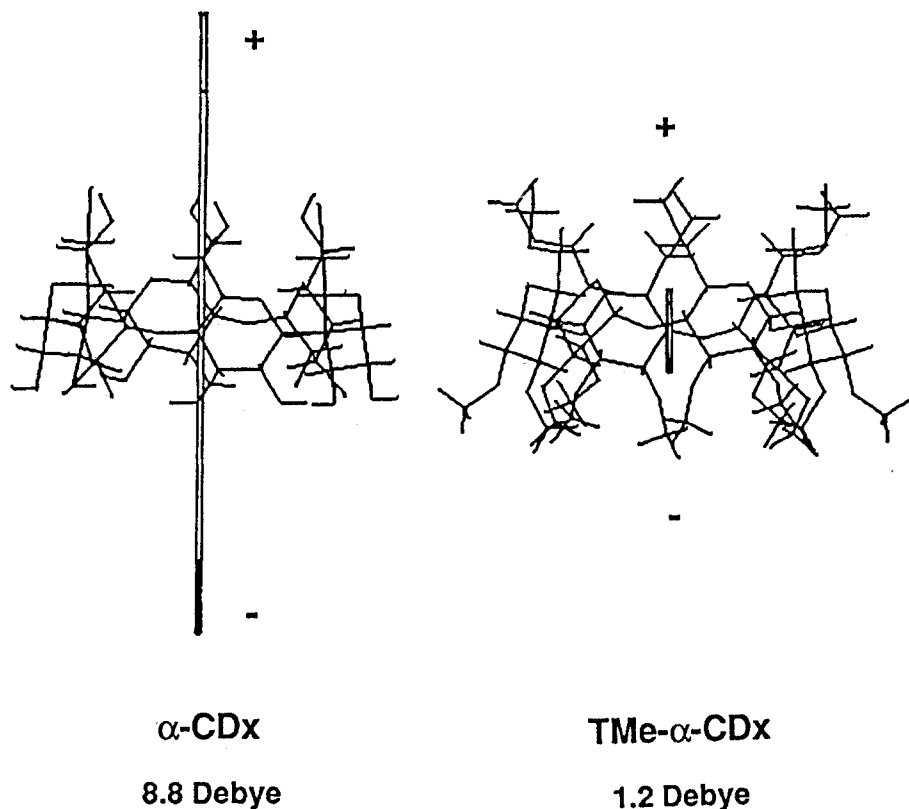


Fig. 8. Dipole moments of  $\alpha$ -CDx and TMe- $\alpha$ -CDx calculated using a MOPAC software.

of *p*-TA are shown in Figure 9. The up-field shifts of the signals due to the protons at the 2- and 3-positions and downfield shift of the signals due to the protons at the 5-position are well explained by the anisotropic effect by a benzene ring situated in the fashion shown in Figure 7 (type III). Essentially the same results were obtained for the *p*-TA-TMe- $\alpha$ -CDx system as shown in Figures 10 and 11.

We determined the thermodynamic parameters for complexation. The  $K$  values were determined as a function of temperature and the results are summarized in Table I. Good linear relationships in the van't Hoff plots gave the enthalpy ( $\Delta H$ ) and entropy changes ( $\Delta S$ ) for complexation. The results are also listed in Table I. The complex formation in the *p*-TA- $\alpha$ -CDx system is the enthalpically favorable and entropically unfavorable process. Such enthalpically dominated complexation has been interpreted in terms of the van der Waals interaction as a main binding force [5, 7]. On the contrary, the complexation of *p*-TA with TMe- $\alpha$ -CDx shows a negative and relatively small  $\Delta H$  and a positive and large  $\Delta S$ . Such entropically dominated complexation of *p*-TA with TMe- $\alpha$ -CDx cannot be explained by ordinary hydrophobic effects. Previously, we found that the formation of the complex of 3-(*p*-hydroxyphenyl)-1-propanol and TMe- $\beta$ -CDx is the enthalpically favor-

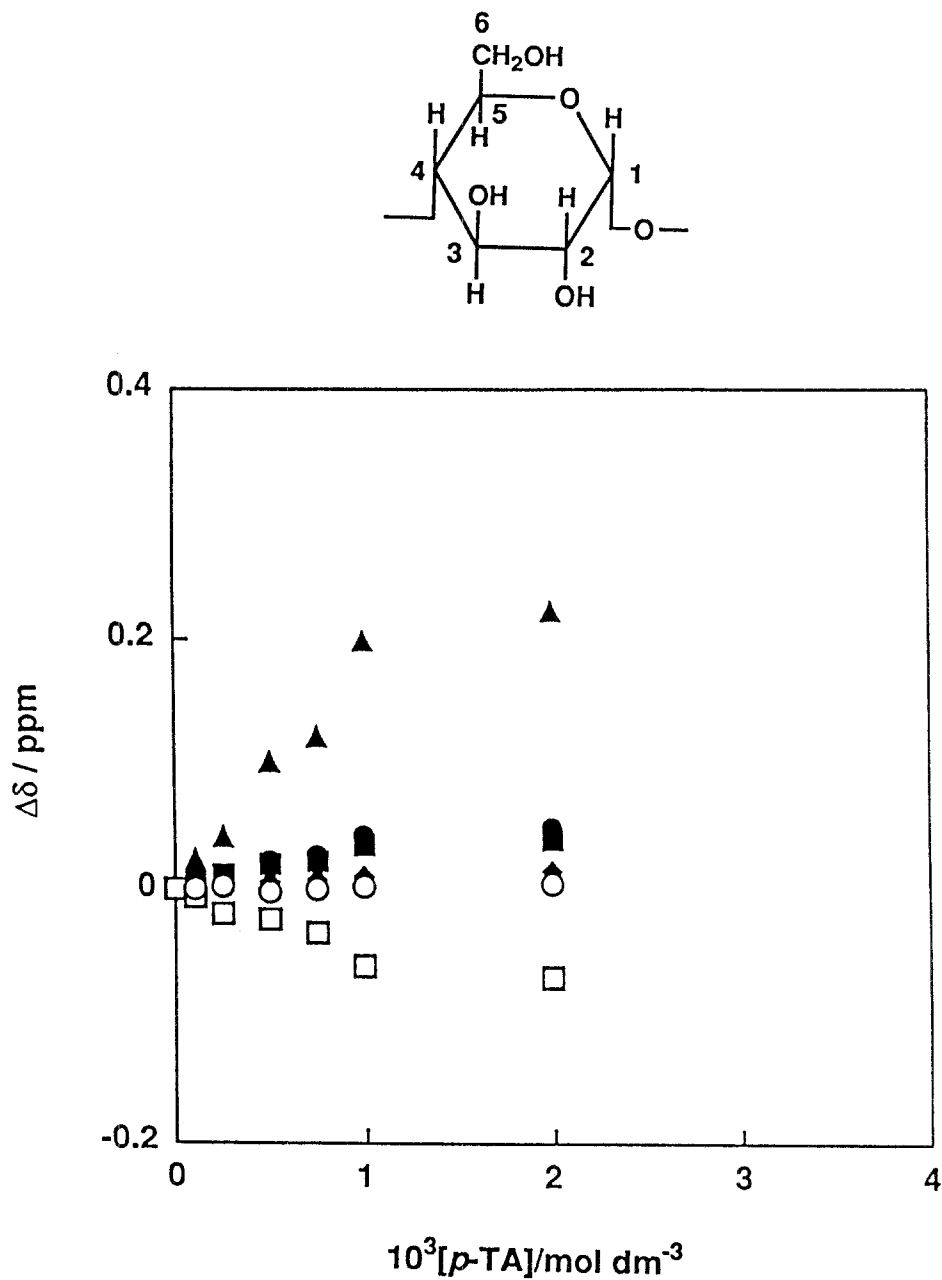


Fig. 9. Changes in the chemical shifts of  $\alpha$ -CDx ( $1 \times 10^{-3} \text{ mol dm}^{-3}$ ) upon addition of  $p$ -TA in D<sub>2</sub>O at pD 2.0. ■: H-1; ●: H-2; ▲: H-3; ◆: H-4; □: H-5; ○: H-6.

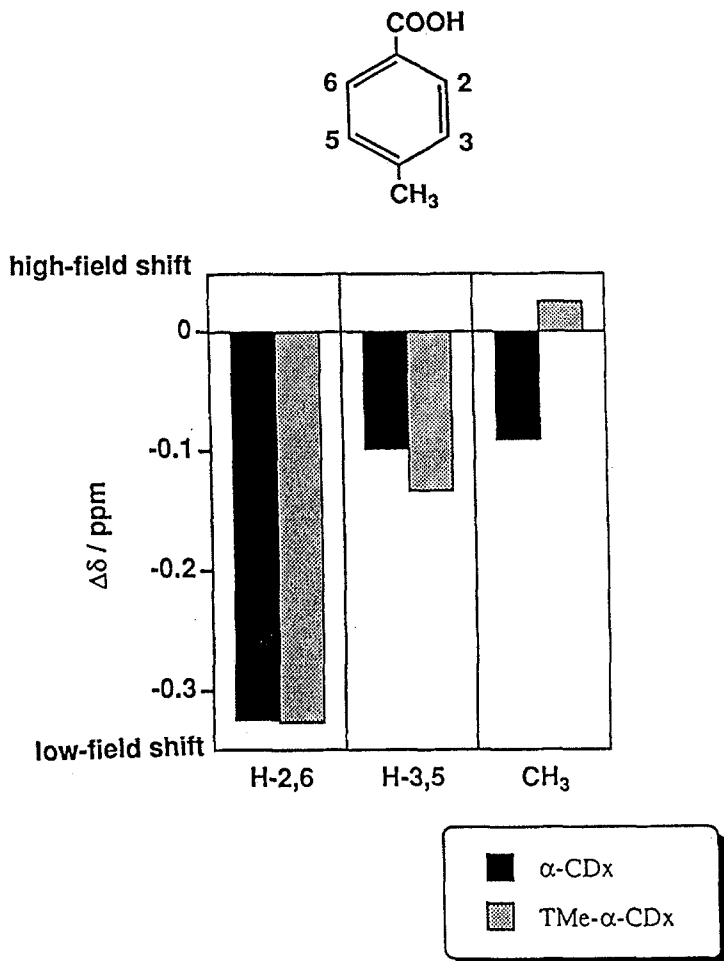


Fig. 10. Changes in the chemical shifts of *p*-TA ( $1 \times 10^{-3}$  mol dm $^{-3}$ ) upon addition of  $\alpha$ -CDx and TMe- $\alpha$ -CDx ( $8 \times 10^{-3}$  mol dm $^{-3}$ ) in D<sub>2</sub>O at pD 2.0.

able and entropically unfavorable process [9]. 3-(*p*-Hydroxyphenyl)-1-propanol is more hydrophobic than *p*-TA. The inclusion of *p*-TA in the TMe- $\alpha$ -CDx cavity may provide (1) dehydration from both host and guest molecules, (2) reduction in the conformational and translational freedom of both host and guest molecules, (3) dipole-dipole interaction between host and guest, and (4) van der Waals interaction between host and guest. In these phenomena, only dehydration from *p*-TA and TMe- $\alpha$ -CDx can lead to the positive  $\Delta S$ . On the basis of our previous results [9], it is very hard to conclude that the positive  $\Delta S$  in the present system is dominantly ascribed to the dehydration from TMe- $\alpha$ -CDx. As the  $^1\text{H}$  NMR data indicate, the CO<sub>2</sub>H group of *p*-TA penetrates into the hydrophobic host cavity from the wider side of the CDx toroid to form the type III complex. This process requires extended

## high-field shift

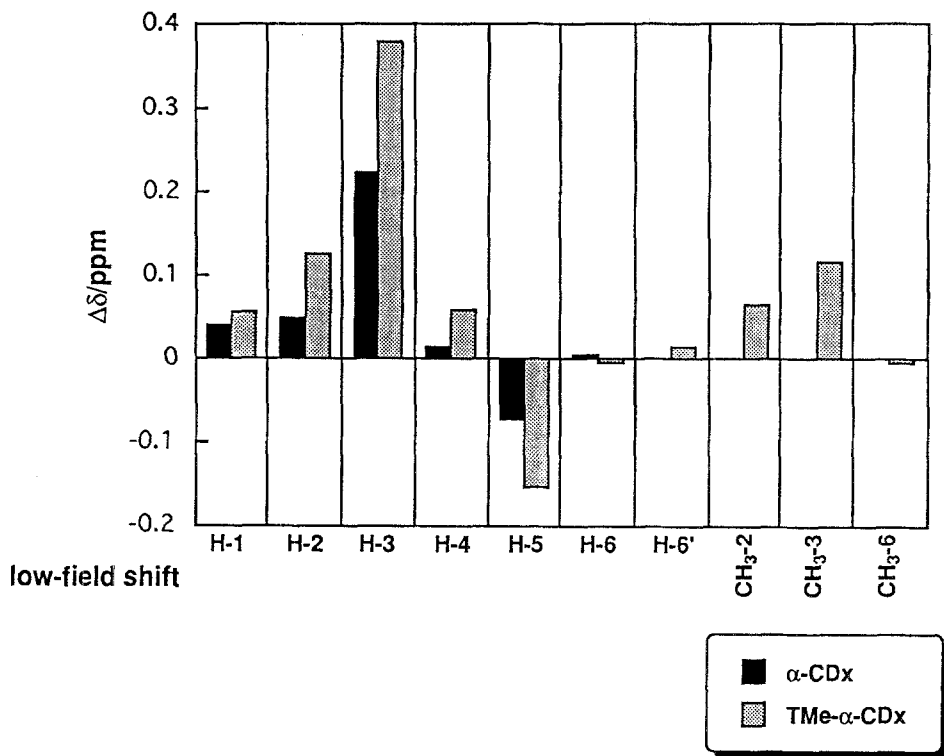


Fig. 11. Changes in the chemical shifts of  $\alpha$ -CDx and TMe- $\alpha$ -CDx ( $1 \times 10^{-3}$  mol dm $^{-3}$ ) upon addition of *p*-TA ( $3 \times 10^{-3}$  mol dm $^{-3}$ ) in D<sub>2</sub>O at pD 2.0.

dehydration from the polar CO<sub>2</sub>H group leading to increase in the freedom of the system. Since the structure of the *p*-TA- $\alpha$ -CDx complex is essentially the same as that of the *p*-TA-TMe- $\alpha$ -CDx one, the dehydration from the CO<sub>2</sub>H group of *p*-TA should also occur in this system. In this case, however, the strong van der Waals interaction may overcome the effect of the dehydration. The inflexible nature of the  $\alpha$ -CDx cavity due to the intramolecular hydrogen bonding seems to provide stronger van der Waals contacts between the host and guest molecules. A negative and large  $\Delta H$  may cause the negative and large  $\Delta S$  in the *p*-TA- $\alpha$ -CDx system. Such an enthalpy-entropy compensation effect is generally observed in inclusion phenomena of CDxs [16]. We concluded that the type I complex is formed in the *o*-TA-TMe- $\alpha$ -CDx system. In this complex, a part of the CO<sub>2</sub>H group is exposed to the aqueous bulk phase. Therefore, the dehydration from this CO<sub>2</sub>H group is less strict than that of the type III complex. This should be the reason for the positive but small  $\Delta S$  in the *o*-TA-TMe- $\alpha$ -CDx system.

## Acknowledgment

This work was supported by a Grant-in-Aid for Science Research from the Ministry of Education, Science and Culture of Japan. We are indebted to Nayo Okumura for her experimental assistance.

## References

1. (a) K. Harata: *J. Incl. Phenom.* **1**, 279 (1984). (b) K. Harata, F. Hirayama, H. Arima, K. Uekama, and T. Miyaji: *J. Chem. Soc., Perkin Trans. 2*, 1159 (1992).
2. K. Harata, K. Uekama, M. Otagiri, and F. Hirayama: *Bull. Chem. Soc. Jpn.* **60**, 497 (1987).
3. K. Harata, K. Uekama, M. Otagiri, and F. Hirayama: *Bull. Chem. Soc. Jpn.* **55**, 3904 (1982).
4. Y. Inoue, Y. Takahashi, and R. Chûjô: *Carbohydr. Res.* **144**, C9 (1985).
5. K. Harata, K. Tsuda, K. Uekama, M. Otagiri, and F. Hirayama: *J. Incl. Phenom.* **6**, 135 (1988).
6. K. Harata: *Bioorg. Chem.* **10**, 255 (1981).
7. E. S. Hall and H. J. Ache: *J. Phys. Chem.* **83**, 1805 (1979).
8. E. A. Lewis and L. D. Hansen: *J. Chem. Soc., Perkin Trans. 2* 2081 (1973).
9. K. Kano, Y. Tamiya, and S. Hashimoto: *J. Incl. Phenom.* **13**, 287 (1992).
10. S. Hakomori: *J. Biochem. (Tokyo)* **55**, 205 (1964).
11. T. Yorozu, M. Hoshino, and M. Imamura: *J. Phys. Chem.* **86**, 4422 (1982).
12. R. J. Bergeron, M. A. Channing, and K. A. McGovern: *J. Am. Chem. Soc.* **100**, 2878 (1978).
13. K. Harata: *Bull. Chem. Soc. Jpn.* **50**, 1416 (1977).
14. R. I. Gelb, L. M. Schwartz, R. F. Johnson, and D. A. Laufer: *J. Am. Chem. Soc.* **101**, 1869 (1979).
15. (a) K. Kano, K. Mori, B. Ueno, M. Goto, and T. Kubota: *J. Am. Chem. Soc.* **112**, 8645 (1990). (b) M. Kitagawa, H. Hoshi, M. Sakurai, Y. Inoue, and R. Chûjô: *Bull. Chem. Soc. Jpn.* **61**, 4225 (1988). (c) R. I. Gelb, L. M. Schwartz, B. Cardelino, H. S. Fuhrman, R. F. Johnson, and D. A. Laufer: *J. Am. Chem. Soc.* **103**, 1750 (1981).
16. Y. Inoue, T. Hakushi, Y. Liu, L.-H. Tong, B.-J. Shen, and D.-S. Jin: *J. Am. Chem. Soc.* **115**, 475 (1993).